



OPEN

Genomic analysis of plasma circulating tumor DNA in patients with heavily pretreated HER2 + metastatic breast cancer

Kyoungmin Lee^{1,19}, Jongwon Lee^{2,3,19}, Jungmin Choi^{3,4}, Sung Hoon Sim⁵, Jeong Eun Kim⁶, Min Hwan Kim⁷, Yeon Hee Park⁸, Jee Hyun Kim⁹, Su-Jin Koh¹⁰, Kyong Hwa Park¹¹, Myoung Joo Kang¹², Mi Sun Ahn¹³, Kyoung Eun Lee¹⁴, Hee-Jun Kim¹⁵, Hee Kyung Ahn¹⁶, Han Jo Kim¹⁷, Keon Uk Park¹⁸ & In Hae Park^{1✉}

We explored accumulated genomic alterations in patients with heavily treated HER2 + metastatic breast cancer enrolled in the KCSG BR18-14/KM10B trial. Targeted sequencing was performed with circulating tumor DNAs (ctDNAs) collected before the treatment of 92 patients. ctDNAs collected at the time of disease progression from seven patients who had a durable response for > 12 months were also analyzed. Sixty-five genes were identified as pathogenic alterations in 99 samples. The most frequently altered genes were *TP53* (n = 48), *PIKCA* (n = 21) and *ERBB3* (n = 19). *TP53* and *PIK3CA* mutations were significantly related with shorter progression free survival (PFS), and patients with a higher ctDNA fraction showed a worse PFS. The frequency of homologous recombination deficiency (HRD)-related gene mutations was higher than that in matched tumor tissues, and these mutations tended to be associated with shorter PFS. New pathogenic variants were found at the end of treatment in all seven patients, including *BRCA2*, *VHL*, *RAD50*, *RB1*, *BRIP1*, *ATM*, *FANCA*, and *PIK3CA* mutations. In conclusion, *TP53* and *PIK3CA* mutations, as well as a higher ctDNA fraction, were associated with worse PFS with trastuzumab and cytotoxic chemotherapy. The enrichment of HRD-related gene mutations and newly detected variants in ctDNA may be related to resistance to treatment.

¹Division of Oncology/Hematology, Department of Internal Medicine, Korea University Guro Hospital, Korea University College of Medicine, Seoul, Korea. ²Brain Korea 21 Plus Project for Biomedical Science, Korea University College of Medicine, Seoul, Korea. ³Department of Biomedical Sciences, Korea University College of Medicine, Seoul, Korea. ⁴Department of Genetics, Yale University School of Medicine, New Haven, CT, USA. ⁵Center for Breast Cancer, National Cancer Center, Goyang, Korea. ⁶Department of Oncology, Asan Medical Center, University of Ulsan College of Medicine, Seoul, Korea. ⁷Division of Medical Oncology, Department of Internal Medicine, Yonsei Cancer Center, Yonsei University College of Medicine, Seoul, Korea. ⁸Division of Hematology/Oncology, Department of Medicine, Samsung Medical Center, Sungkyunkwan University School of Medicine, Seoul, Korea. ⁹Department of Internal Medicine, Seoul National University Bundang Hospital, Seoul National University College of Medicine, Seongnam, Korea. ¹⁰Department of Hematology and Oncology, Ulsan University Hospital, Ulsan University College of Medicine, Ulsan, Korea. ¹¹Division of Oncology/Hematology, Department of Internal Medicine, Korea University Anam Hospital, Korea University College of Medicine, Seoul, Korea. ¹²Division of Oncology, Department of Internal Medicine, Haeundae Paik Hospital, Inje University College of Medicine, Busan, Korea. ¹³Department of Hematology-Oncology, Ajou University School of Medicine, Suwon, Korea. ¹⁴Department of Hematology and Oncology, Ewha Womans University Hospital, Seoul, Korea. ¹⁵Division of Hematology/Medical Oncology, Department of Internal Medicine, Chung-Ang University Hospital, Seoul, Korea. ¹⁶Division of Medical Oncology, Department of Internal Medicine, Gachon University Gil Medical Center, Incheon, Korea. ¹⁷Division of Oncology and Hematology, Department of Internal Medicine, Soonchunhyang University Cheonan Hospital, Cheonan, Korea. ¹⁸Division of Hematology/Oncology, Department of Internal Medicine, Keimyung University Dongsan Hospital, Daegu, Korea. ¹⁹These authors contributed equally: Kyoungmin Lee and Jongwon Lee. ✉email: parkih@korea.ac.kr

HER2-positive breast carcinomas are known to exhibit HER2 amplification, which drives many oncogenic processes in cancer cells¹. Currently, diverse anti-HER2 drugs have been developed, and are the standard treatment strategies for HER2-positive metastatic breast cancer (HER2 + MBC). Currently, dual anti-HER2 blockade antibodies (trastuzumab and pertuzumab) with cytotoxic chemotherapy and anti-HER2 antibody–drug conjugates (ADCs) [fam-trastuzumab-deruxtecan (T-Dxd) or trastuzumab emtansine (T-DM1)] are commonly recommended as first- or second-line therapies for HER2 + MBC^{2,3}. For subsequent lines, anti-HER2 tyrosine kinase inhibitors, engineered antibodies, or the reuse of trastuzumab with different chemotherapy partners is suggested based on the concept of a continuum of anti-HER2 therapy⁴.

However, there is insufficient data and no consensus on how many times anti-HER2 therapy can be applied. Various acquired resistances accumulated through multiple treatments are expected in heavily pretreated patients, and tumor clonal evolution under therapeutic pressure may alter the genomic characteristics of primary tumor cells^{5–7}. So far, there are few data regarding genetic alterations in heavily pretreated HER2 + MBC. New treatment options could be obtained for these populations by identifying the genetic alterations associated with treatment resistance.

Tissue-based next-generation sequencing (NGS) remains the gold standard for tumor genomic characterization⁸; however, the invasiveness of multiple tissue biopsies is a major hurdle, especially for heavily treated patients. Furthermore, the analysis of tumor tissue is limited in representing intra- and inter-tumor heterogeneity, which is the main cause of treatment resistance^{9,10}. Blood-based liquid biopsy for detecting circulating tumor DNA (ctDNA) is an attractive alternative that can provide a heterogeneous picture of tumors and track dynamic genomic changes in an easy and safe manner^{11,12}.

In this study, we explored the accumulated genomic alterations and their clinical significance through ctDNA analysis in patients with heavily treated HER2 + MBC using blood samples from patients who were enrolled in the KCSG BR18-14/KM10B trial.

Results

Overview of targeted sequencing of ctDNA results. In the present study, 100 peripheral blood samples were collected from 93 patients. The ctDNA data of 99 samples were included in the final analysis, as one sample that failed the Quality Control (QC) checks was excluded. Overall, 92 samples were obtained at the time of screening and paired end of-treatment (EOT) samples were obtained from seven patients. One patient failed to provide blood samples during screening, and only the EOT sample was collected. Of the 93 patients, 31 also provided FFPE tumor tissues (Supplementary Table S1). The clinical characteristics of the patient records included in the final dataset are presented in Table 1.

	N = 93
Age (years, median, range)	54 (20–70)
Menstruation status	
Premenopausal	32 (34.4%)
Postmenopausal	60 (64.5%)
Unknown	1 (1.1%)
HR status	
HR (+)	53 (57.0%)
HR (–)	37 (39.8%)
Unknown	3 (3.2%)
De novo stage IV	29 (31.2%)
No. of prior chemotherapy regimens at metastatic setting* (median, range)	
1–3	35 (38.0%)
> 3	57 (62.0%)
Unknown	1 (1.1%)
No. of prior anti-HER2 therapy at metastatic setting** (median, range)	
1–3	71 (76.3%)
> 3	22 (23.7%)
Prior anti-HER2 agents	
Trastuzumab	90 (96.8%)
Pertuzumab	39 (41.9%)
Trastuzumab emtansine (T-DM1)	90 (96.8%)
Lapatinib	70 (75.3%)
Trastuzumab deruxtecan (T-Dxd)	9 (9.7%)

Table 1. Patients' characteristics. *HR* hormone receptor, *No.* number. *Number of all administered chemotherapies regardless of anti-HER2 drugs in a metastatic setting. **Number of anti-HER2 based treatments in a metastatic setting.

DNA isolated from plasma samples and tumor tissues was subjected to hybridization capture and targeted deep sequencing to detect somatic single-nucleotide variants (SNVs), small insertions and deletions (indels), and copy number alterations. The average concentration of ctDNA was 1.18 ng/ μ L (range 0.16–10.23 ng/ μ L) from 99 samples. A summary of targeted sequencing data is presented in Supplementary Tables S2 and S3. The mean target coverage for tissue samples was 809.25x (range, 176.7–1538.45x) and 4710x (range 1851–7161x) for plasma samples. Overall, a median of 96.4% and 99.6% of the target bases were satisfied, with a coverage of more than 100 \times in tissue and plasma samples, respectively. This result indicated that we obtained adequate coverage of the target genes to detect genomic alterations with high sensitivity.

Mutational landscape and prevalence of pathogenic variants in ctDNA. To examine the prevalence and relevance of any detected pathogenic variants in the ctDNA, a mutational landscape was generated from 99 ctDNA samples (Fig. 1A). After removing variants from the germline, blacklist, and clonal hematopoiesis, 336 pathogenic somatic alterations and 25 copy number alterations were identified in 65 genes (Supplementary Tables S4–S7). *TP53* was the most frequently altered gene (48 out of 99 samples), followed by *PIK3CA* ($n=21$), *ERBB3* ($n=19$), *ATM* ($n=17$), *RAD50* ($n=16$), *ERBB2* ($n=15$), *ARID1A* ($n=12$), and *BRCA2* ($n=11$). This pattern is comparable to that observed in previous studies on breast cancer^{13,14}.

The ctDNA fractions were further calculated to evaluate their utility as prognostic biomarkers in qualified samples. Of the 99 plasma samples, 85 were calculated using the maximum allelic fraction of the pathogenic variants, and the remaining 14 samples were excluded from the analysis because of the absence of a pathogenic variant. The median ctDNA fraction was 3.33%, and its distribution is shown in Supplementary Table S8 and Fig. 1B.

Concordance of genetic alterations between ctDNAs and matched tumor tissues. Of the 31 patients who had both plasma samples and matched tumor tissues, 135 genes were found to have somatic alterations in either sample. To determine the concordance between tissue and plasma samples, our analysis specifically concentrated on 61 genes that were covered by both the CancerSCAN and the Axen panel (Supplementary Table S9). The median time interval between tumor and plasma sample collection was 42 months (range 2–104 months). Sixteen of the 31 patients had 26 concordant alterations in both samples, including 18 SNVs, three indels, and five amplifications (Fig. 2 and Supplementary Table S10). The gene-level variant concordance rate between the tissue and ctDNA samples ranged from 73.8% (45/61) to 95.1% (58/61), including all alterations present or absent. *TP53* (10/31, 32.3%) showed the highest concordance rate at the gene level, followed by *PIK3CA* (7/31, 22.6%), ranged from 0% (0/31) to 32.3% (10/31), which is comparable to those reported in other breast cancer studies^{15,16}.

We further analyzed several factors that could affect the concordance rate, such as the time of tumor tissue acquisition (primary or metastatic tissue), time interval between tissue and plasma sample collection, and ctDNA fraction. The concordance rate was not significantly different according to the time of tumor tissue acquisition or the time interval between tissue and plasma collection (data not shown). The ctDNA fraction of the concordant group ($n=16$) was significantly higher than that of the discordant group ($n=15$) (Supplementary Fig. S1 and Supplementary Table S8). This result suggests that a higher ctDNA fraction was a major factor in the concordance between plasma and tissue, which is consistent with the reports of previous studies^{15,17}.

Enrichment of HRD-related gene mutations in ctDNA. We found that pathogenic alterations in HRD-related genes, including *ATM*, *RAD50*, *BRCA1/2*, *BRIP1*, *PALB2*, *BARD1* and *CHEK2* were enriched in ctDNA analysis data (Fig. 1). Therefore, we investigated whether the detection rate of HRD-related gene mutations differed between the tumor tissue and ctDNA from 31 pairs of samples. Most variants detected in ctDNA had AF as low as <1%; however, the total number of pathogenic variants was higher in ctDNA. Among them, HRD-related gene mutations represented 7.1% (2 of 28 pathogenic alterations) of the tumor samples and 31.1% (51 of 164 pathogenic alterations) of the ctDNA samples (Fig. 3).

Survival analyses according to the ctDNA genetic alterations. Survival analysis was performed using data from 89 patients with survival information for the study treatment. With a median follow-up duration of 12.7 months (95% CI 10.3–15.1), the median PFS and OS of all 89 patients was 4.6 (95% CI 4.0–5.2) and 19.7 (95% CI 11.8–27.6) months, respectively. As shown in Fig. 4, *PIK3CA* (median 2.9 vs. 5.6 months, HR=2.07, 95% CI 1.17–3.68, $p=0.010$) and *TP53* (median 3.3 vs. 5.8 months, HR=2.17, 95% CI 1.35–3.47, $p<0.001$) mutations were significantly associated with shorter PFS. A higher ctDNA fraction (>3.33% [median]) was also associated with a worse PFS (median 3.3 vs. 5.9 months, HR=1.95, 95% CI 1.25–3.05, $p=0.003$). *PIK3CA* mutation, *TP53* mutation, and higher ctDNA fraction were associated with poor OS (median 12.6 vs. 22.9 months, $p=0.012$; 12.6 vs. 19.7 months, $p=0.002$; 12.6 vs. 22.9 months, $p=0.001$, respectively). The prognostic value of *TP53* and *PIK3CA* mutations, as well as ctDNA fractions, remained consistent after adjusting for age (≤ 55 years vs >55 years), number of prior anti-HER2 therapies (≤ 3 vs >3), and presence of visceral metastasis (no vs yes) (Supplementary Table S11). *ERBB2* amplification was detected in only 15 patients, and patients with *ERBB2* amplification had worse PFS (median 3.4 vs. 4.9 months, HR=2.11, 95% CI 1.04–4.31, $p=0.034$). Of note, patients with HRD gene mutations tended to have shorter PFS, although this was not statistically significant (median 3.2 vs. 4.9 months, HR=1.66, 95% CI 0.91–3.03, $p=0.09$) (Supplementary Fig. S2).

Post-treatment clonal evolutions detected by paired sample analyses. To identify the potential mechanisms of treatment resistance, we examined pathogenic variants from six patients who had paired ctDNA (Initial and EOT) (Fig. 5). These six patients had PFS longer than 12 months; therefore, we hoped to identify the mechanisms of acquired resistance from the analysis of samples from these patients. Three of the patients

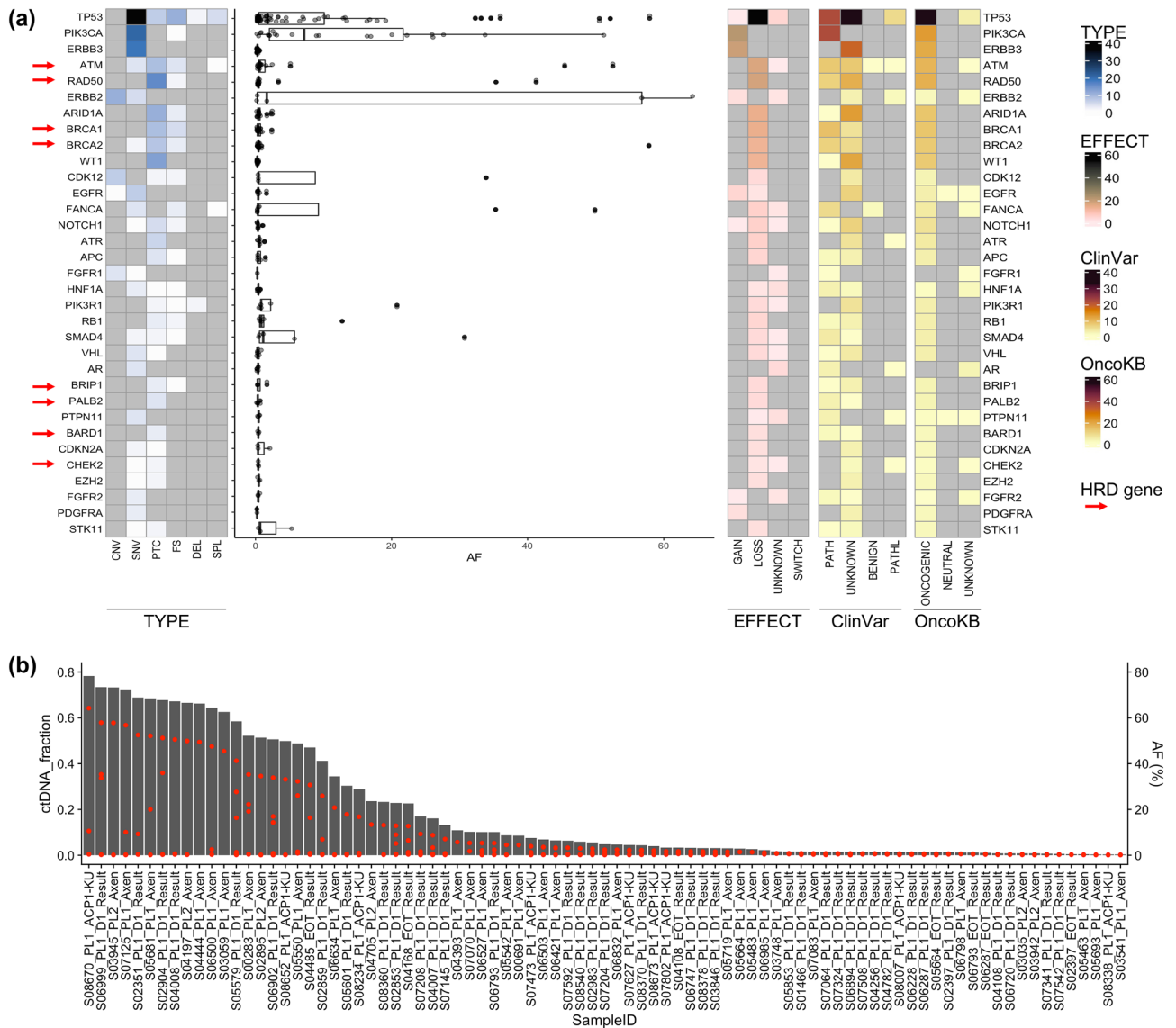


Figure 1. Genomic landscape of ctDNA in patients with metastatic breast cancer. **(a)** Mutational landscape represented by top 33 frequently mutated genes. More than two variants are identified on both sides of the figure. The heat map shows the number of variants of the top mutated genes referring to the mutation type (left), different functional classes, or pathogenicity (right). The distribution of allelic fractions of each variant is shown in a boxplot with jitter (center). Red arrows indicate the HRD genes. **(b)** ctDNA fraction (%; gray bars) calculated using pathogenic variants allelic fraction (Red dots) from the quantifiable 85 samples. HRD, homologous recombination deficiency. Variant annotations were defined as follows. Mutation type: CNV, Copy number variation; SNV, Missense_variant, splice_region_variant; PTC, stop_gained&splice_region_variant, stop_gained; FS: frameshift_variant, frameshift_variant&stop_gained, frameshift_variant&splice_region_variant; DEL, conservative_inframe_deletion, disruptive_inframe_deletion, splice_donor_variant&disruptive_inframe_deletion&splice_region_variant&intron_variant; SPL, splice_acceptor_variant&intron_variant, splice_donor_variant&intron_variant, splice_region_variant, and intron_variant. EFFECT (functional classes)—GAIN, Gain_of_function, Likely Gain-of-function; LOSS, Loss of function; Likely Loss of function; SWITCH, Switch-of-function, Likely Switch-of-function; UNKNOWN, Unknown ClinVar-PATH, pathogenic, pathogenic/likely pathogenic; PATHL, Likelypathogenic; BENIGN, Benign; UNKNOWN, Conflicting_interpretations_of_pathogenicity, Uncertain_significance, not_provided. OncoKB-ONCOGENIC, oncogenic, likely oncogenic, predicted oncogenic; NEUTRAL, likely neutral; UNKNOWN, unknown; NA.

(S06287, S06793, and S02397) also had tumor tissue samples. For S06287, the *PIK3CA_E542K* mutation was detected in both the tumor tissue and initial ctDNA. However, this was not observed in the EOT sample, instead revealing previously undetected *BRCA2* and *CDK12* mutations. In S04485, the *PIK3CA_E542K* mutation was not initially found; however, it was detected with high AF at EOT. In addition, pathogenic HRD-related gene mutations were found in EOT samples, except for S02397, including *BRCA2*, *RAD50*, *ATM*, *FANCA*, and *BRIP1*.

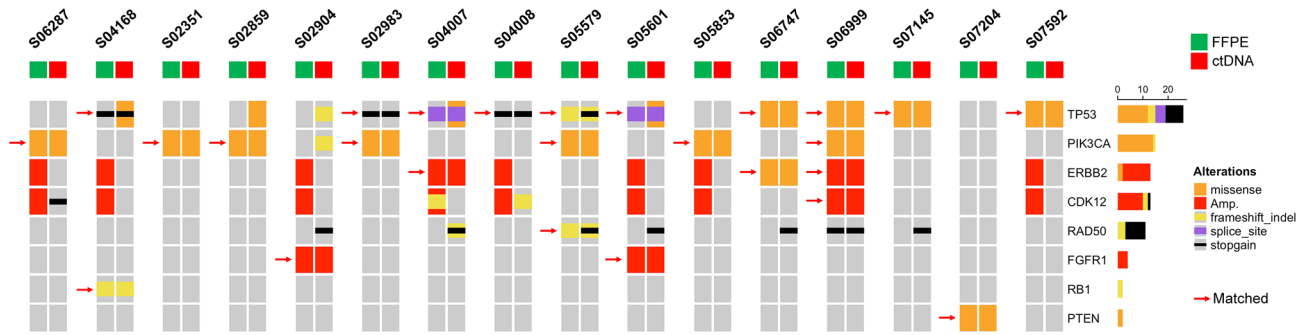


Figure 2. Oncoprint chart for top 8 genes from 16 patients who had shared 26 alterations in both tissue and plasma samples. Concordant gene alterations detected in both biopsies are indicated by red arrows. Green and red squares on the top represent tissue and plasma samples, respectively.

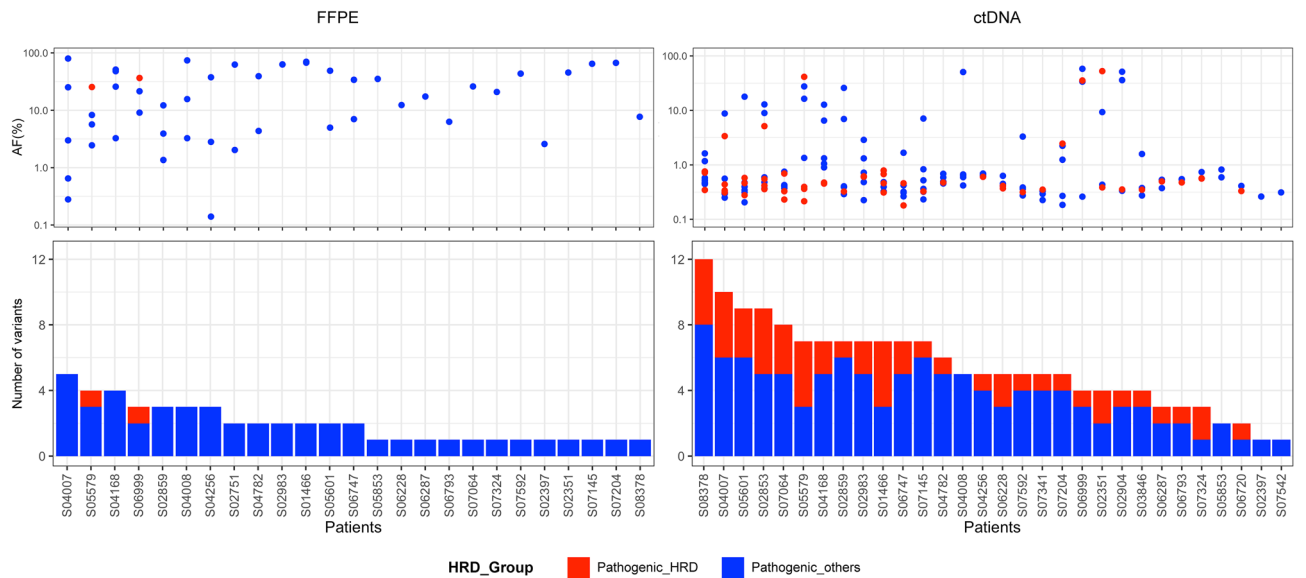


Figure 3. Enrichment of HRD-related gene mutation in ctDNA. Distribution of pathogenic variant allelic fraction and number of variants detected in FFPE or ctDNA samples. HRD homologous recombination deficiency, FFPE formalin fixed paraffin embedded.

Discussion

HER2 overexpression in HER2 + breast cancer is an important oncogenic driver and therapeutic target; however, its genetic heterogeneity is known to be an important resistance mechanism to anti-HER2 therapy^{18–20}. Moreover, due to tumor evolution and treatment pressure, genomic alterations in metastatic breast cancer can differ substantially from those in the primary tumor and become more disparate after multiple lines of chemotherapy^{7,21}. In this study, we demonstrated the genomic landscape of ctDNA in patients with HER2 + MBC whose disease progressed after multiple lines of standard HER2-directed chemotherapy.

Consistent with previous studies^{22,23}, *TP53* and *PIK3CA* mutations were the two most altered genes. It is well known that the frequency of *TP53* mutation is especially high in HER2 + breast cancer, and *TP53* mutation per se is associated with early onset breast cancer and poor prognosis²⁴. Recently, Liu et al. demonstrated the potential of *TP53* mutation as a biomarker for predicting the efficacy of anti-HER2 therapies, including antibody-based drugs and TKIs, through ctDNA analysis²⁵. In our study, patients with *TP53* mutations had worse PFS and OS. Although the predictive role of *TP53* mutations cannot be justified due to the limitation of the single-arm study design, the development of targeting *TP53* mutations seems necessary for patients with worse prognosis. Aberrant activation of PI3K is also a well-known oncogenic driver in breast cancer, including the HER2 + subtype, and is one of the major resistance mechanisms in anti-HER2 therapy²⁶. A previous study showed that patients with HER2 + breast cancer with an activating *PIK3CA* mutation had lower pathologic complete response (pCR) rates and shorter PFS with palliative HER2-targeted therapy²⁷. *PIK3CA* mutations in plasma ctDNA also predict survival and treatment outcomes in various types of advanced cancers²⁸, and a recent meta-analysis validated this finding in breast cancer²⁹. In our study, patients with *PIK3CA* mutations in ctDNA showed a low treatment response and poor survival outcomes. In addition, *PIK3CA* pathogenic mutation with high AF was detected in the ctDNA when the disease progressed in one patient, indicating a possible therapeutic target for this patient.

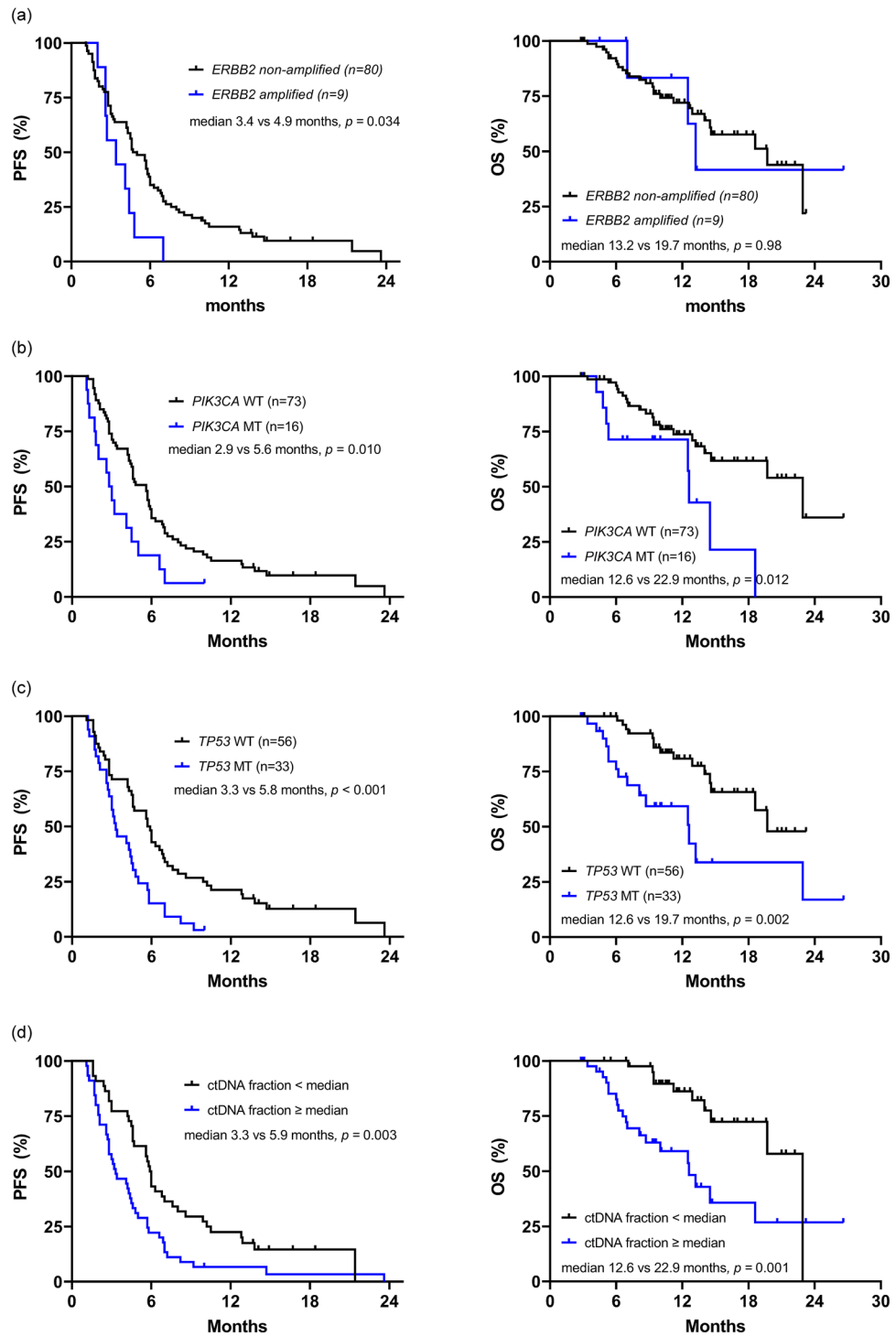


Figure 4. Kaplan–Meier estimates of progression free survival and overall survival on study treatment according to (a) *ERBB2* amplification, (b) *PIK3CA* mutation, (c) *TP53* mutation, and (d) ctDNA fraction. PFS progression free survival, OS overall survival.

Currently, many clinical trials using PIK3CA inhibitors with anti-HER2 therapy are ongoing, and these studies are expected to inform the role of PIK3CA inhibitors in HER2 + breast cancer²⁶. Beyond detecting single gene alterations, we calculated the ctDNA fraction and demonstrated its possible role as a prognostic biomarker in HER2 + MBC. ctDNA is assumed to reflect the tumor burden and has been suggested as a tool for prognostication and follow-up in patients with advanced cancers^{30,31}. Several studies have shown the prognostic ability of ctDNA fractions in patients with MBC^{22,23}, and a recent study advocated its role as a pragmatic, independent prognostic biomarker across the four most common advanced cancer types, including MBC, in real-world

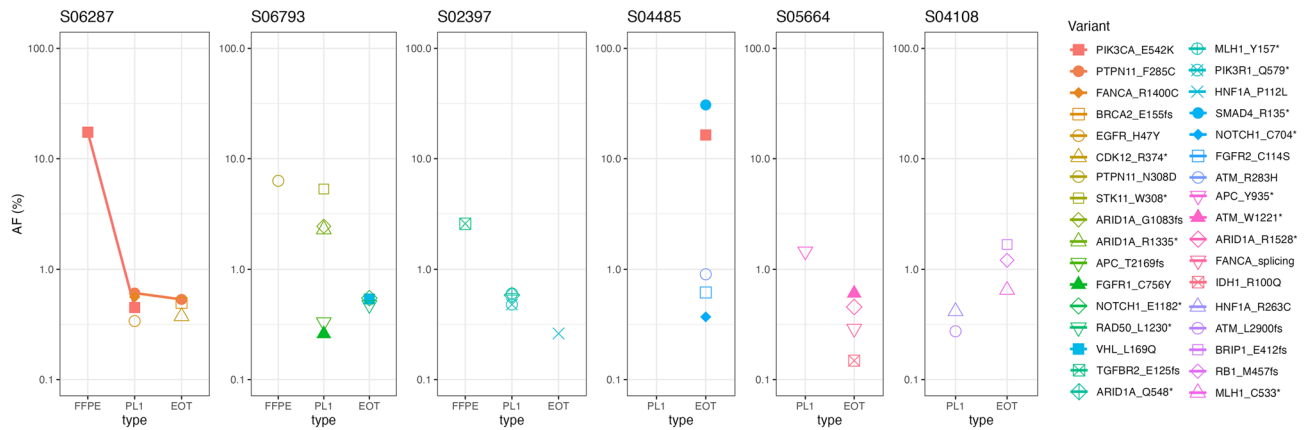


Figure 5. Changes in allelic fraction of pathogenic variants detected in FFPE or serial ctDNA samples. *PL1* ctDNA at initial treatment, *EOT* ctDNA at end of treatment.

settings³². Moreover, although not addressed in our study, several studies have found that early on-treatment ctDNA dynamics were a surrogate for treatment outcomes^{33,34}. However, many issues need to be addressed before applying ctDNA fractions in actual clinical practice, such as panel sensitivity, standard formula for calculating ctDNA fraction, and reliable cut-off values.

Interestingly, our findings showed that mutations of HRD-related genes were more frequent in ctDNA than in tumor tissue, and patients with HRD-related gene mutations tended to have shorter PFS. Additionally, various pathogenic HRD gene mutations have been detected in EOT samples collected during disease progression. There is limited data suggesting the accumulation of alterations in HRD-related genes during multiple chemotherapy cycles. However, considering the functional aspects of HRD-related genes, this enrichment suggests the presence of tumor cells that can survive despite impaired DNA repair mechanisms caused by prior anticancer therapy. And these tumor cells are likely to be resistant to subsequent treatments. Further studies are needed to determine whether they can be targeted.

In our study, *ERBB2* (*HER2*) amplification was detected in 15 patients (16%) and was reanalyzed and confirmed by droplet digital PCR (data not shown). The positive rate of *HER2* in ctDNA is significantly lower than the previously reported 33–96% for metastatic *HER2* + breast cancer and 9–31% for early breast cancer^{35,36}. The low detection of *ERBB2* in ctDNA could potentially be attributed to the previous anti-*HER2* treatment effects. However, it would be challenging to draw definitive conclusions without confirming the presence of *ERBB2* amplification in corresponding tumor cells. Our results reveal an intriguing association between *ERBB2* amplification in ctDNA and poor PFS. Assuming that low levels of *ERBB2* in ctDNA resulted from prior anti-*HER2* treatment, the persistent high detection of *ERBB2* in ctDNA suggests a potential resistance to anti-*HER2* therapy. This observation aligns with the results of the phase III KATHERINE study where high *HER2* RNA expression in residual tumors after trastuzumab containing neoadjuvant treatment was associated with worse outcomes in the trastuzumab adjuvant treatment group³⁷. Additionally, the CALGB40601 study reported worse relapse free survival associated with the *HER2* enriched subtype in residual disease following neoadjuvant treatment including trastuzumab ± lapatinib³⁸. Considering these findings, the persistent high detection of *ERBB2* amplification in ctDNA may serve as a potential biomarker of anti-*HER2* therapy, warranting further validation in future studies. Our study was conducted as a translational study parallel to a prospective clinical trial but had some limitations. First, no tumor tissue collected at the same time point could be compared with the ctDNA analysis results. Therefore, newly detected variants, including *ERBB2* amplification, in ctDNA could not be confirmed. Second, there was a considerable time interval between tissue and plasma sample collection. The relatively low concordance may be due to tumor evolution occurring over such a long time, but this needs to be verified further. Finally, we did not collect serial follow-up ctDNA samples from all patients. Therefore, data on the association between ctDNA dynamics and treatment effect could not be obtained.

In conclusion, *TP53* and *PIK3CA* mutation and a higher ctDNA fraction were associated with worse PFS and OS in patients with heavily treated *HER2* + MBC. Accumulation of mutations in HRD-related genes was noted in the ctDNA analysis and was related to shorter PFS. ctDNA analysis can be useful for predicting the efficacy of anti-*HER2* treatment and patient prognosis, even in heavily pretreated populations. It can also provide valuable information regarding new therapeutic targets for these patients.

Methods

Patient cohort and sample collection. The KCSG BR18-14/KM10B trial was a multicenter, single-arm, phase 2 study that investigated the efficacy and safety of a trastuzumab biosimilar, Herzuma®, in combination with the treatment of physician's choice (TPC) in patients with *HER2* + MBC who had failed 2 or more *HER2* directed chemotherapies³⁹. The median PFS and OS were 4.6 months (95% CI 2.8–7.2) and 18.6 months (95% CI 14.4–not reached), respectively. For exploratory biomarker analysis, blood samples (pre-treatment/disease progression) and/or formalin-fixed paraffin-embedded (FFPE) tumor tissues (primary or metastatic) were obtained from all participants (n = 110). Among them, 17 patients who failed to provide ctDNA were excluded for this

analysis. For the blood samples, 10 mL of whole blood was collected with Cell-Free DNA BCT® for ctDNA preparation. Written informed consent was obtained from each patient prior to performing all study procedures. This study was approved by the Institutional Review Board of the Korea University Guro Hospital (IRB number 2019GR0420) and conducted in accordance with the guidelines for Good Clinical Practice and the Declaration of Helsinki.

NGS and genomic analysis. Targeted sequencing of tumor tissues and ctDNAs was carried out with the K-MASTER project, a Korean solid cancer genome analysis research project⁴⁰. Targeted sequencing using tumor tissues were performed using CancerSCAN™ (Samsung Genome Institute, Seoul, Korea) which encompasses the exons of 396 human cancer related genes (Supplementary Table S12). In the case of ctDNA analysis, we utilized the K-Master Axen™ Cancer Panel (Macrogen, Seoul, Korea) targeting the exons of 89 human cancer related genes (Supplementary Table S13)⁴¹. DNA input for generate sequencing library was 200 ng for FFPE and 10 ng for ctDNA samples. Paired-end 150 bp reads were generated on a HiSeq2500 or NovaSeq6000 sequencing system (Illumina, San Diego, CA, USA). Detailed methods for targeted sequencing and data processing were the same as previous reports except removing frequently detected variants that are likely to be alignment artifacts (blacklists) and germline variants⁴⁰.

ClinVar (Pathogenic or Likely-pathogenic) or OncoKB (Oncogenic or Likely-oncogenic) database were referred to identify the pathogenic mutations. To exclude the influence of clonal hematopoiesis related variants, hematopoietic-associated gene mutations were further investigated via literature review^{42,43} and COSMIC database.

Concordance was defined at the single-gene level as detection of an identical alteration, as previously described¹⁶. The ctDNA fraction was estimated based on the allelic fraction of somatic mutations as described⁴⁴ but relying on a modified approach as measured by the maximum somatic mutant allele fraction (MSAF)¹⁴. Homologous recombination deficiency (HRD) was defined as germline or somatic pathogenic alterations of the following 11 genes: *BRCA1*, *BRCA2*, *ATM*, *BARD1*, *BRIP1*, *CHEK2*, *PALB2*, *RAD51B*, *RAD51C*, *RAD51D*, and *RAD50*, as previous reports^{45–47}.

Statistical analysis. Patient demographics and genomic alterations were summarized using descriptive statistics. The Wilcoxon signed-rank test was used to evaluate statistical differences in ctDNA fractions between the concordant and discordant groups. To determine the clinical significance of specific genetic alterations, the progression-free survival (PFS) and overall survival (OS) of the study treatment were analyzed. Survival curves were generated with GraphPad Prism 5 (GraphPad Software, San Diego, CA, USA) using the Kaplan–Meier method and compared using the log-rank test. In the survival analysis, a mutation with an allele frequency (AF) of $\geq 1\%$ was defined as positive^{48,49}. All other statistical analyses were performed using R version 4.0.3 (R Foundation for Statistical Computing, Vienna, Austria), and statistical significance was two-tailed, with a significance set at $P \leq 0.05$.

Ethics approval statement. This study was approved by the Institutional Review Board of the Korea University Guro Hospital (IRB number 2019GR0420) and conducted in accordance with the guidelines for Good Clinical Practice and the Declaration of Helsinki.

Data availability

The data generated in this study are available within the article and its supplementary data files, and further inquiries can be directed to the corresponding authors.

Received: 13 April 2023; Accepted: 25 May 2023

Published online: 19 June 2023

References

- Allegretti, M. *et al.* Liquid biopsy identifies actionable dynamic predictors of resistance to Trastuzumab Emtansine (T-DM1) in advanced HER2-positive breast cancer. *Mol. Cancer* **20**, 151. <https://doi.org/10.1186/s12943-021-01438-z> (2021).
- Gradishar, W. J. *et al.* NCCN Guidelines® insights: Breast cancer, version 4.2021. *J. Natl. Compr. Canc. Netw.* **19**, 484–493. <https://doi.org/10.6004/jnccn.2021.0023> (2021).
- Gennari, A. *et al.* ESMO Clinical Practice Guideline for the diagnosis, staging and treatment of patients with metastatic breast cancer. *Ann. Oncol.* **32**, 1475–1495. <https://doi.org/10.1016/j.annonc.2021.09.019> (2021).
- Nader-Marta, G., Martins-Branco, D. & de Azambuja, E. How we treat patients with metastatic HER2-positive breast cancer. *ESMO Open* **7**, 100343. <https://doi.org/10.1016/j.esmoop.2021.100343> (2022).
- Venkatesan, S., Swanton, C., Taylor, B. S. & Costello, J. F. Treatment-induced mutagenesis and selective pressures sculpt cancer evolution. *Cold Spring Harb. Perspect Med.* **7**, a026617. <https://doi.org/10.1101/cshperspect.a026617> (2017).
- Li, A., Schleicher, S. M., Andre, F. & Mitri, Z. I. Genomic alteration in metastatic breast cancer and its treatment. *Am. Soc. Clin. Oncol. Educ. Book* **40**, 1–14. https://doi.org/10.1200/edbk_280463 (2020).
- Angus, L. *et al.* The genomic landscape of metastatic breast cancer highlights changes in mutation and signature frequencies. *Nat. Genet.* **51**, 1450–1458. <https://doi.org/10.1038/s41588-019-0507-7> (2019).
- Ilyas, M. Next-generation sequencing in diagnostic pathology. *Pathobiology* **84**, 292–305. <https://doi.org/10.1159/000480089> (2017).
- Muciño-Olmos, E. A. *et al.* Unveiling functional heterogeneity in breast cancer multicellular tumor spheroids through single-cell RNA-seq. *Sci. Rep.* **10**, 12728. <https://doi.org/10.1038/s41598-020-69026-7> (2020).
- Parikh, A. R. *et al.* Liquid versus tissue biopsy for detecting acquired resistance and tumor heterogeneity in gastrointestinal cancers. *Nat. Med.* **25**, 1415–1421. <https://doi.org/10.1038/s41591-019-0561-9> (2019).
- Heitzer, E., Haque, I. S., Roberts, C. E. S. & Speicher, M. R. Current and future perspectives of liquid biopsies in genomics-driven oncology. *Nat. Rev. Genet.* **20**, 71–88. <https://doi.org/10.1038/s41576-018-0071-5> (2019).

12. Chae, Y. K. *et al.* Concordance between genomic alterations assessed by next-generation sequencing in tumor tissue or circulating cell-free DNA. *Oncotarget* **7**, 65364–65373. <https://doi.org/10.18632/oncotarget.11692> (2016).
13. Hu, Z. Y. *et al.* Identifying circulating tumor DNA mutation profiles in metastatic breast cancer patients with multiline resistance. *EBioMedicine* **32**, 111–118. <https://doi.org/10.1016/j.ebiom.2018.05.015> (2018).
14. Kingston, B. *et al.* Genomic profile of advanced breast cancer in circulating tumour DNA. *Nat. Commun.* **12**, 2423. <https://doi.org/10.1038/s41467-021-22605-2> (2021).
15. Xu, B. *et al.* Concordance of genomic alterations between circulating tumor DNA and matched tumor tissue in Chinese patients with breast cancer. *J. Oncol.* **2020**, 4259293. <https://doi.org/10.1155/2020/4259293> (2020).
16. Chae, Y. K. *et al.* Concordance of genomic alterations by next-generation sequencing in tumor tissue versus circulating tumor DNA in breast cancer. *Mol. Cancer Ther.* **16**, 1412–1420. <https://doi.org/10.1158/1535-7163.Mct-17-0061> (2017).
17. Tukachinsky, H. *et al.* Genomic analysis of circulating tumor DNA in 3334 patients with advanced prostate cancer identifies targetable BRCA alterations and AR resistance mechanisms. *Clin. Cancer Res.* **27**, 3094–3105. <https://doi.org/10.1158/1078-0432.Ccr-20-4805> (2021).
18. Ferrari, A. *et al.* A whole-genome sequence and transcriptome perspective on HER2-positive breast cancers. *Nat. Commun.* **7**, 12222. <https://doi.org/10.1038/ncomms12222> (2016).
19. Chen, B. *et al.* Heterogeneity of genomic profile in patients with HER2-positive breast cancer. *Endocr. Relat. Cancer* **27**, 153–162. <https://doi.org/10.1530/erc-19-0414> (2020).
20. de Oliveira Taveira, M. *et al.* Genomic characteristics of trastuzumab-resistant Her2-positive metastatic breast cancer. *J. Cancer Res. Clin. Oncol.* **143**, 1255–1262. <https://doi.org/10.1007/s00432-017-2358-x> (2017).
21. Brown, D. *et al.* Phylogenetic analysis of metastatic progression in breast cancer using somatic mutations and copy number aberrations. *Nat. Commun.* **8**, 14944. <https://doi.org/10.1038/ncomms14944> (2017).
22. Liao, H. *et al.* Identification of mutation patterns and circulating tumour DNA-derived prognostic markers in advanced breast cancer patients. *J. Transl. Med.* **20**, 211. <https://doi.org/10.1186/s12967-022-03421-8> (2022).
23. Liu, B. *et al.* The circulating tumor DNA (ctDNA) alteration level predicts therapeutic response in metastatic breast cancer: Novel prognostic indexes based on ctDNA. *Breast* **65**, 116–123. <https://doi.org/10.1016/j.breast.2022.07.010> (2022).
24. Fedorova, O. *et al.* Attenuation of p53 mutant as an approach for treatment Her2-positive cancer. *Cell Death Discov.* **6**, 100. <https://doi.org/10.1038/s41420-020-00337-4> (2020).
25. Liu, B. *et al.* Molecular landscape of TP53 mutations in breast cancer and their utility for predicting the response to HER-targeted therapy in HER2 amplification-positive and HER2 mutation-positive amplification-negative patients. *Cancer Med.* **11**, 2767–2778. <https://doi.org/10.1002/cam4.4652> (2022).
26. Rasti, A. R. *et al.* PIK3CA mutations drive therapeutic resistance in human epidermal growth factor receptor 2-positive breast cancer. *JCO Precis. Oncol.* **6**, e2100370. <https://doi.org/10.1200/po.21.00370> (2022).
27. Kim, J. W. *et al.* PIK3CA mutation is associated with poor response to HER2-targeted therapy in breast cancer patients. *Cancer Res. Treat.* <https://doi.org/10.4143/crt.2022.221> (2022).
28. Dumbrava, E. E. *et al.* PIK3CA mutations in plasma circulating tumor DNA predict survival and treatment outcomes in patients with advanced cancers. *ESMO Open* **6**, 100230. <https://doi.org/10.1016/j.esmoop.2021.100230> (2021).
29. Galvano, A. *et al.* The diagnostic accuracy of PIK3CA mutations by circulating tumor DNA in breast cancer: An individual patient data meta-analysis. *Ther. Adv. Med. Oncol.* **14**, 17588359221110162. <https://doi.org/10.1177/17588359221110162> (2022).
30. Strijker, M. *et al.* Circulating tumor DNA quantity is related to tumor volume and both predict survival in metastatic pancreatic ductal adenocarcinoma. *Int. J. Cancer* **146**, 1445–1456. <https://doi.org/10.1002/ijc.32586> (2020).
31. Nygaard, A. D., Holdgaard, P. C., Spindler, K. L. G., Pallisgaard, N. & Jakobsen, A. The correlation between cell-free DNA and tumour burden was estimated by PET/CT in patients with advanced NSCLC. *Br. J. Cancer* **110**, 363–368. <https://doi.org/10.1038/bjc.2013.705> (2014).
32. Reichert, Z. R. *et al.* Prognostic value of plasma circulating tumor DNA fraction across four common cancer types: A real-world outcomes study. *Ann. Oncol.* **34**, 111–120. <https://doi.org/10.1016/j.annonc.2022.09.163> (2023).
33. Hrebien, S. *et al.* Early ctDNA dynamics as a surrogate for progression-free survival in advanced breast cancer in the BEECH trial. *Ann. Oncol.* **30**, 945–952. <https://doi.org/10.1093/annonc/mdz085> (2019).
34. Ma, F. *et al.* Assessing tumor heterogeneity using ctDNA to predict and monitor therapeutic response in metastatic breast cancer. *Int. J. Cancer* **146**, 1359–1368. <https://doi.org/10.1002/ijc.32536> (2020).
35. Verschoor, N. *et al.* Validity and utility of HER2/ERBB2 copy number variation assessed in liquid biopsies from breast cancer patients: A systematic review. *Cancer Treat Rev.* **106**, 102384. <https://doi.org/10.1016/j.ctrv.2022.102384> (2022).
36. Zhao, W. *et al.* Receptor conversion impacts outcomes of different molecular subtypes of primary breast cancer. *Ther. Adv. Med. Oncol.* **13**, 17588359211012982. <https://doi.org/10.1177/17588359211012982> (2021).
37. Denkert, C. *et al.* Biomarker data from the phase III KATHERINE study of adjuvant T-DM1 versus trastuzumab for residual invasive disease after neoadjuvant therapy for HER2-positive breast cancer. *Clin. Cancer Res.* **29**, 1569–1581. <https://doi.org/10.1158/1078-0432.Ccr-22-1989> (2023).
38. Fernandez-Martinez, A. *et al.* Survival, pathologic response, and genomics in CALGB 40601 (Alliance), a neoadjuvant phase III trial of paclitaxel-trastuzumab with or without lapatinib in HER2-positive breast cancer. *J. Clin. Oncol.* **38**, 4184–4193. <https://doi.org/10.1200/JCO.20.01276> (2020).
39. Sim, S. H. *et al.* Phase II study to investigate the efficacy of trastuzumab biosimilar (Herzuma[®]) plus treatment of physician's choice (TPC) in patients with heavily pretreated HER-2+ metastatic breast cancer (KCSG BR 18–14/KM10B). *Breast* **65**, 172–178. <https://doi.org/10.1016/j.breast.2022.08.002> (2022).
40. Lee, Y. *et al.* Clinical application of targeted deep sequencing in metastatic colorectal cancer patients: Actionable genomic alteration in K-MASTER project. *Cancer Res. Treat* **53**, 123–130. <https://doi.org/10.4143/crt.2020.559> (2021).
41. Choi, Y. J. *et al.* Comparison of the data of a next-generation sequencing panel from K-MASTER project with that of orthogonal methods for detecting targetable genetic alterations. *Cancer Res. Treat* **54**, 30–39. <https://doi.org/10.4143/crt.2021.218> (2022).
42. Guermouche, H. *et al.* High prevalence of clonal hematopoiesis in the blood and bone marrow of healthy volunteers. *Blood Adv.* **4**, 3550–3557. <https://doi.org/10.1182/bloodadvances.2020001582> (2020).
43. Feusier, J. E. *et al.* Large-scale identification of clonal hematopoiesis and mutations recurrent in blood cancers. *Blood Cancer Discov.* **2**, 226–237. <https://doi.org/10.1158/2643-3230.Bcd-20-0094> (2021).
44. Vandekerckhove, G. *et al.* Circulating tumor DNA reveals clinically actionable somatic genome of metastatic bladder cancer. *Clin. Cancer Res.* **23**, 6487–6497. <https://doi.org/10.1158/1078-0432.Ccr-17-1140> (2017).
45. Park, W. *et al.* Genomic methods identify homologous recombination deficiency in pancreas adenocarcinoma and optimize treatment selection. *Clin. Cancer Res.* **26**, 3239–3247. <https://doi.org/10.1158/1078-0432.Ccr-20-0418> (2020).
46. Nguyen, L., J, W. M. M., Van Hoeck, A. & Cuppen, E. Pan-cancer landscape of homologous recombination deficiency. *Nat. Commun.* **11**, 5584. <https://doi.org/10.1038/s41467-020-19406-4> (2020).
47. Yamamoto, H. & Hirasawa, A. Homologous recombination deficiencies and hereditary tumors. *Int. J. Mol. Sci.* **23**, 348. <https://doi.org/10.3390/ijms23010348> (2021).
48. Wang, J. F. *et al.* Variants with a low allele frequency detected in genomic DNA affect the accuracy of mutation detection in cell-free DNA by next-generation sequencing. *Cancer* **124**, 1061–1069. <https://doi.org/10.1002/cncr.31152> (2018).

49. Shu, Y. *et al.* Circulating tumor DNA mutation profiling by targeted next generation sequencing provides guidance for personalized treatments in multiple cancer types. *Sci. Rep.* 7, 583. <https://doi.org/10.1038/s41598-017-00520-1> (2017).

Acknowledgements

We thank the patients and their families, as well as the investigators in KCSG Breast Committee.

Author contributions

K.L. and J.L.: methodology, formal analysis, validation, writing—original draft; C.J.: methodology, formal analysis, investigation; S.H.S., J.E.K., M.H.K., Y.H.P., J.H.K., S.-J.K., K.H.P., M.J.K., M.S.A., K.E.L., H.-J.K., H.K.A., H.J.K. and K.E.P.: data collection, resources; I.H.P.: conceptualization, methodology, writing—review and editing, project administration. All authors have read and approved the manuscript, and I.H.P. is responsible for submitting the manuscript for publication.

Funding

This research was supported by a grant of the Korea University College of Medicine (grant number: K2107471), and a grant of the Korea Health Technology R&D Project through the Korea Health Industry Development Institute (KHIDI) funded by the Ministry of Health & Welfare, Republic of Korea (grant number: HI17C2206).

Competing interests

The authors declare no competing interests.

Additional information

Supplementary Information The online version contains supplementary material available at <https://doi.org/10.1038/s41598-023-35925-8>.

Correspondence and requests for materials should be addressed to I.H.P.

Reprints and permissions information is available at www.nature.com/reprints.

Publisher's note Springer Nature remains neutral with regard to jurisdictional claims in published maps and institutional affiliations.



Open Access This article is licensed under a Creative Commons Attribution 4.0 International License, which permits use, sharing, adaptation, distribution and reproduction in any medium or format, as long as you give appropriate credit to the original author(s) and the source, provide a link to the Creative Commons licence, and indicate if changes were made. The images or other third party material in this article are included in the article's Creative Commons licence, unless indicated otherwise in a credit line to the material. If material is not included in the article's Creative Commons licence and your intended use is not permitted by statutory regulation or exceeds the permitted use, you will need to obtain permission directly from the copyright holder. To view a copy of this licence, visit <http://creativecommons.org/licenses/by/4.0/>.

© The Author(s) 2023